Antenna Array for a 24-GHz Automotive Radar with Dipole Antenna Element Patches

Johan Wernehag and Henrik Sjöland
Department of Electroscience
Lund University
Box 118, 221 00 Lund Sweden
Email: {Johan.Wernehag, Henrik.Sjoland}@es.lth.se

Abstract

In this paper 3D electromagnetic simulations of an antenna array have been performed. The array is intended for automotive radar applications at 24 GHz. It is constructed from dipole antenna element patches, which are fed in the center by a differential signal.

The dipole antenna element patches are simulated assuming a standard off the shelf substrate. They have a standing wave ratio less than 3 from 22.5 GHz to 24.5 GHz, when matched to 60 Ω. The directivity of the dipole patch is 9 dBi.

The array consists of 24 elements giving it a physical size of 150 mm, with a groundplane of 200×100 mm^2. An antenna of that size is easy to integrate in a car. Beam steering can be accomplished by changing the phases of the signals to the different elements [1], thus making the arrangement mechanically robust since the antenna does not have to move. The directivity for the antenna array is larger than 9.4 dBi for a steering angle of ±7° and the half power beam width is smaller than 6° over the same steering angle.

1. Introduction

The car industry and the legislators are very interested in an automotive radar system. The injuries from car collisions cost the society a lot both in medical bills and in human tragedies. In the United States (US) alone motor vehicle crashes accounted for 42,000 deaths, more than 5.3 million injuries, and over $231 billion in economic losses in 2000 [2].

Today there are already automotive radars available [3]–[5]. These system are either based on microwave signals or laser. Today's systems add about $1,500 - $3,000 to the cost of a car [3]. This is too much if the radar is going to be an every car commodity and thus decrease the injuries, deaths, and the cost of car crashes. The price tag is why the focus in [1] was directed to digital CMOS processes, which are predicted by International Technology Roadmap for Semiconductors (ITRS) to have transition frequencies (f_T) and maximum oscillation frequencies (f_{max}) in excess of 200 GHz and 310 GHz, respectively, in the coming 5-10 years [6]. This will enable implementation of automotive radar systems at 77 GHz in CMOS. At 77 GHz there is a frequency band allocated both in Europe [7], Japan [8], and the US [9]. The European Telecommunications Standards Institute (ETSI) also has a temporary standard [10] for Short Range Radar (SRR) operating in the frequency band from 24.05 GHz to 24.25 GHz. Furthermore, both ETSI and the Federal Communications Commission (FCC) have a license free Ultra WideBand (UWB) frequency band in this range[1], which can also be used for automotive radar applications. In [1] a 24 GHz automotive radar transmitter circuit topology was presented. The antenna array of this paper is designed to fit that circuit topology.

The chip area in CMOS is relatively cheap compared to III-V devices and the ability to integrate digital signal processing on the same chip as the transmitter further reduces the overall system cost. A typical specification for a 77 GHz radar front end can be seen in Table 1, [4], [8], [11]–[13]. This specification is used for the design at 24 GHz as well since the main antenna[2] requirements are the same.

Table 1: Specification for a 77 GHz front end

Frequency	76-77 GHz
Modulation	FM-CW
Tx Phase Noise	<-80 dBc/Hz @ 100 kHz offset
Bandwidth	300 MHz
Transmit Power	10-15 dBm
Beam Width	4°
Field Of View	8°-20°
Beam Overlap	0.5°
Relative Speed	-200 → +100 km/h
Update Frequency	10 Hz
Range (for 1 m^2 target)	1-100 m

2. Radar Transmitter Circuit

With today's CMOS processes, such as the 130 nm used in [1], 77 GHz is a very high frequency. The aim is therefore set on the 24 GHz frequency band for automotive radar applications.

[1] In the US the ultra wideband is between 22 GHz-29 GHz and in Europe 22.65 GHz-25.65 GHz.

[2] That is the requirement on the resolution is the same and thus the antenna design parameters are the same, such as beam width, field of view, et c

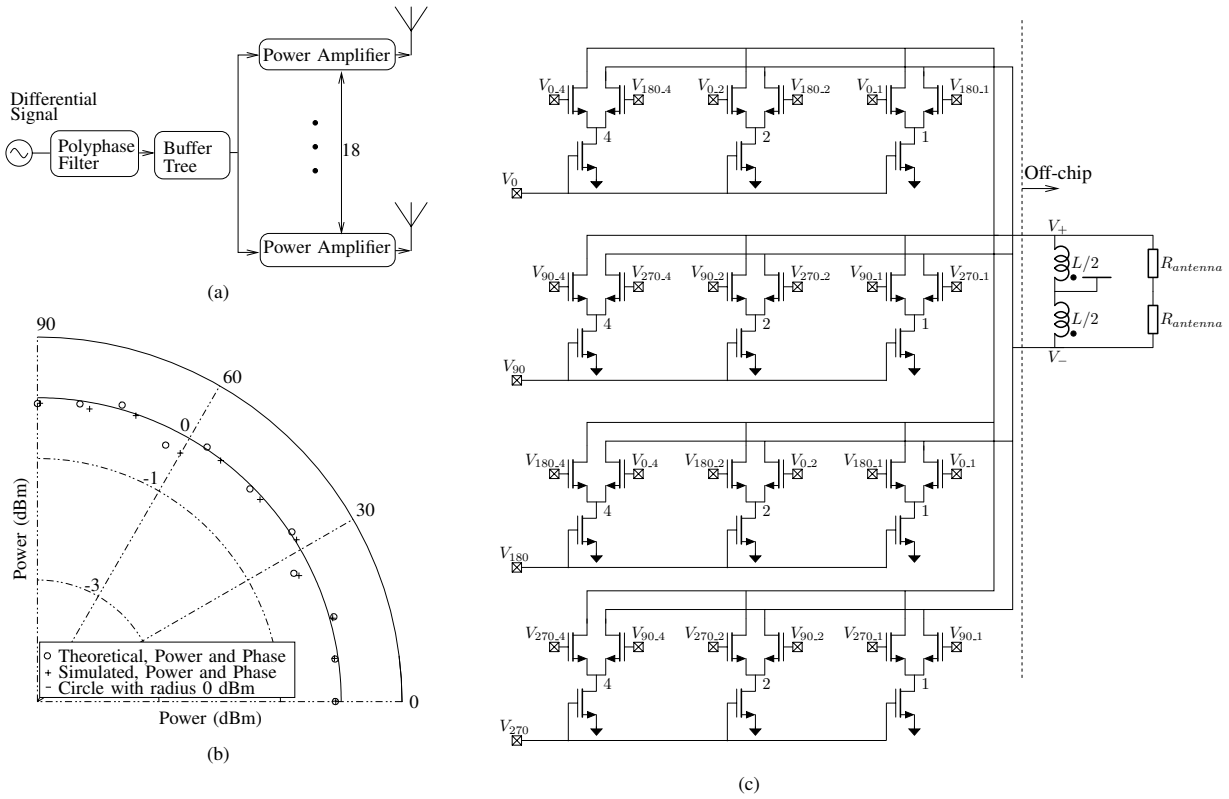

Fig. 1: (a) Block diagram the automotive radar transmitter, (b) The output phasor of a PA swept over one quadrant, (c) Schematic of the power amplifier with three binary weighted transistors per bank

A block diagram of the beam steering multiple Power Amplifier (PA) circuit can be seen in Fig. 1(a).

The PAs in Fig. 1(c) are fed by quadrature signals. A digital control word binary weights the four phases to the output and thus the output phase is controllable through 360°. The simulated phasor tip from one PA is plotted in Fig. 1(b). For a more detailed description of the transmitter see [1].

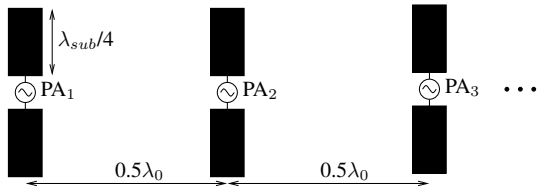

Fig. 2: The dipole patch antenna array with the PA feeding indicated

3. ANTENNA DESIGN

The antenna array must have a high directivity and a small Half Power Beam Width (HPBW) to be able to fulfill a specification like the one in Table 1. In addition, the lobe should be steerable and the antenna mechanically robust. A linear array needs to be at least $10\lambda_0$ to achieve the required HPBW. This has been deduced from ideal radiation expressions [14], hereafter referred to as ideal. That size corresponds to 4 cm at 77 GHz and 13 cm at 24 GHz. A linear array of $\lambda/2$ dipole patches has been assumed, fed in the center by the differential signal from the PAs, see Fig. 2.

The supply voltage to the PAs is inserted at the signal ground at the end of the antenna patches, eliminating the need of separate RF-chokes for feeding the DC-current to the PAs. The physical size of the dipole antenna is roughly $\lambda_{sub}/2$, where λ_{sub} is the wavelength in the substrate. The antenna substrate has a relative dielectric constant of 10.2[3].

To investigate the antenna system further, not assuming ideal expressions, a 3D Electro Magnetic (EM) solver, SEMCAD [15], was used.

First one antenna element was simulated and optimized and later the full array. Broadband simulations were used for the antenna element to investigate its input impedance resonance, field patterns, and surface cur-

[3]This corresponds to substrates available off the shelf, e.g. Arlon AD 1000. The dimensions used in the following section are within the range for this substrate.

rent distributions. Harmonic simulations of the full array were then performed at 24 GHz. To perform broadband simulations of the full array would not be practical, due to excessive computer memory requirements. An advantage of harmonic simulations is that the grid can be made tighter.

A. Antenna Element

The geometry of one patch in a dipole element is defined in Fig. 3(a). The distance between the two patches of the differential antenna element is 100μm. The length, L, of the patch was tuned to give a first resonance at 24 GHz, which occurred for a length equal to 1.3 mm. From this the effective relative dielectric constant at 24 GHz was calculated to be equal to 5.8. The width was chosen to make the input impedance as close as possible to 60 Ω over the frequency band. A wide patch results in a narrow band resonance with a high corresponding impedance. For a narrow patch with a width that is a fraction of the length, the impedance at resonance decreases and multiple resonances occur, thus a more broadband response is attained. A width of 0.6 mm gave the best result, Fig. 4(a-b). At last the thickness of the substrate was investigated to see how thin the substrate could be made. When the thickness was less than 2.8 mm surface waves started to propagate. A substrate thickness of 3.2 mm was therefore chosen to create some margin.

The radiation pattern and surface current distribution for an antenna element with these dimensions are plotted in Fig. 3(b). As seen in Fig. 4(a-b) the input resistance is close to 60 Ω from 22.5 GHz to 24.5 GHz, resulting in a Standing Wave Ration (SWR) less than 3 over that frequency range. The electric field in two vertical cuts for 5 different frequencies is plotted in Fig. 4(c-d). The two cuts are the xz-plane and the yz-plane, according to the coordinate system in Fig. 3(b). As can be seen the directivity is about 9 dBi over the entire frequency range, with a maximum of 10.0 dBi and a minimum of 7.0 dBi, which is in alignment with [16]–[18]. In Fig. 4(d) there is horizontal emission at one frequency, 24.5 GHz. The total simulated ($\eta_{\mathrm{mismatch}} \times \eta_{\mathrm{radiation}}$) antenna element efficiency is 95% at 24 GHz.

B. Antenna Array

The array is made of twentyfour elements with the dimensions found in Section 3-A. A larger substrate of the array than 206×103 mm could not be simulated due to memory limitations (4 GB) of the computer in combination with high requirements on grid resolution.

The three dimensional far-field pattern and surface current distribution is plotted in Fig. 5(a). The antenna efficiency at 2° steering angle is 75%. To validate that the simulation grid is tight enough it has been further tightened without any significant changes in the obtained simulation results. This indicates that the grid is tight enough to predict the far-field behavior correctly. The electric field pattern in the xz- and yz-direction[4] is plotted in Fig. 5(c-d). The field patterns in Fig. 5(c-d) are from 2° and -6° steering angles. The sidelobe supression is larger than 7 dB over the full steering range.

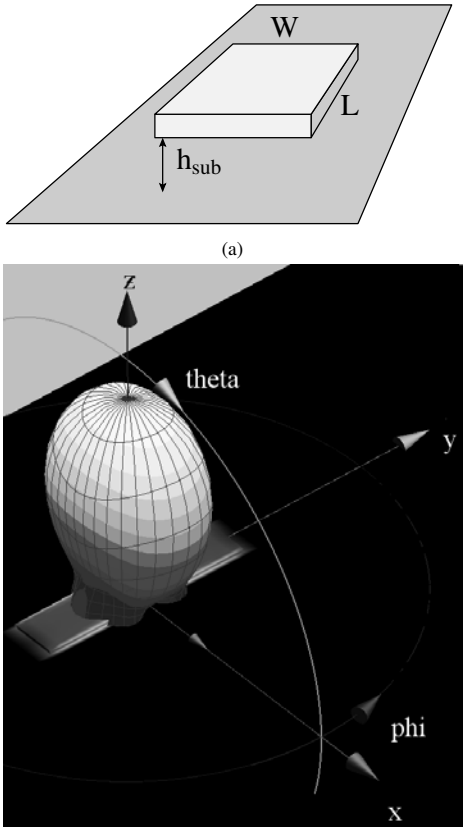

Fig. 3: (a) Geometry of one patch in a dipole element, (b) Radiation pattern and surface current distribution of the element

The directivity ranges from 12.3 dBi at 2° to 9.4 dBi at 4° steering angle. In the yz-direction there are dips of about 10 dB originating from the one dimensional structure of the array. The xz-direction is tilted 13° to align the cut with the first peak in the yz-plane (Fig. 5(a)) for 2° steering angle.

The directivity and HPBW were simulated as a function of steering angle and are plotted in Fig. 5(b). The directivity is larger than 9 dBi and the HPBW is below 6° over the ±7° steering range. A comparison is also made between SEMCAD, Array Pattern Visualizer [19], and the ideal expressions.

4. CONCLUSION

The antenna simulations performed in this paper support the idea that an automotive radar antenna array at 24 GHz can

[4]We use the term direction instead of plane for the array, since when steering out the lobe from zero degrees also the yz-direction of interest will steer out with that angle, theta≠0°. The peak directivity in the xz-direction is not at zero degree either, see the dips in the yz-direction (Fig. 5(d)), so the xz-direction is tilted to the first peak in the yz-direction.

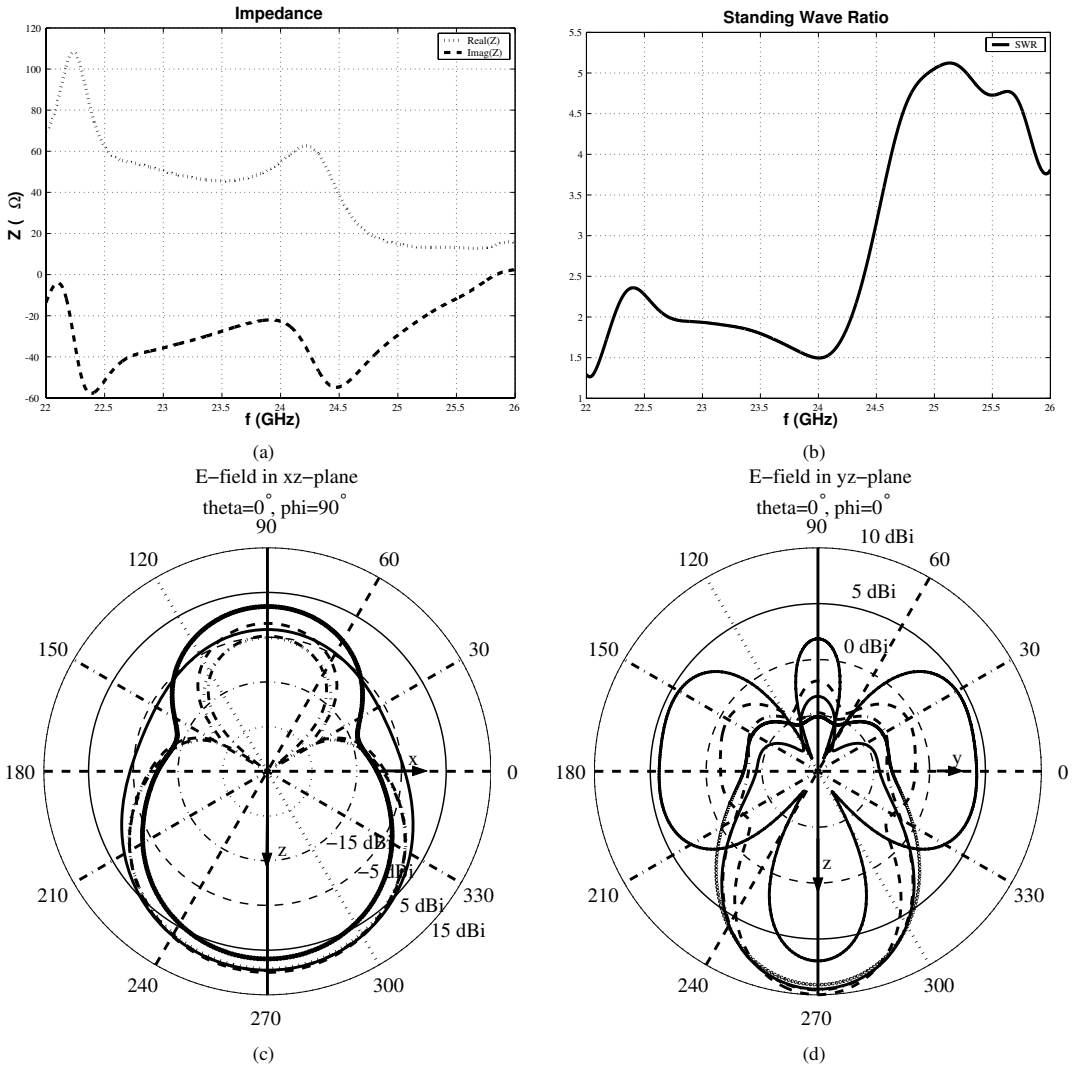

Fig. 4: (a) Input impedance with length 1.3 mm and width 0.6 mm, (b) SWR with length 1.3 mm and width 0.6 mm, (c) and (d) Polar plots of the E-field in vertical cuts at frequencies: 22.5 GHz, 23.0 GHz, 23.5 GHz, 24.0 GHz, and 24.5 GHz

be constructed from dipole patches. The simulated directivity (≈10 dBi) and HPBW (6°) are satisfactory. The physical size of the array is practically implementable in a car (20×10 cm).

Together with the 24 GHz CMOS automotive radar transmitter circuit topology presented by the authors in [1], a low-cost and mechanically robust solution can be accomplished.

ACKNOWLEDGMENT

The authors would also like to thank the Swedish Agency for Innovation Systems (Vinnova) for funding this research, which is a part of the project 'Techniques for Low Cost 60 GHz WLAN'. For SEMCAD introduction and help the authors would like to acknowledge Dr. Anders Johansson.

REFERENCES

[1] J. Wernehag and H. Sjöland, "A 24-GHz Automotive Radar Transmitter with Digital Beam Steering in 130-nm CMOS," *IEEE Ph. D. Research in Microelectronics and Electronics*, pp. 481–484, June 2006.

[2] L. Blincoe, A. Seay, E. Zaloshnja, T. Miller, E. Romano, S. Luchter, and R. Spicer, "The Economic Impact of Motor Vehicle Crashes, 2000," *National Highway Traffic safety Administration*, May 2002, report NO. DOT HS 809 446.

[3] W. D. Jones, "Keeping Cars from Crashing," *IEEE Spectrum*, Sep. 2001.

[4] J. Robinson, D. K. Paul, J. Bird, D. Dawson, T. Brown, D. Spencer, and B. Prime, "A Millimetric Car Radar Front End for Automotive Cruise Control," *IEE Journal Automotive Radar and Navigation Techniques*, no. 1, pp. 1–8, 1998.

[5] G. R. Widmann, M. K. Daniels, L. Hamilton, L. Humm, B. Riley, J. K. Schiffmann, D. E. Schnelker, and W. H. Wishon, "Comparison of Lidar-Based and Radar-Based Adaptive Cruise Control Systems," *SAE Technical Paper Series*, 2000-01-0345.

[6] International Technology Roadmap for Semiconductors (ITRS), http://public.itrs.net/, 2005.

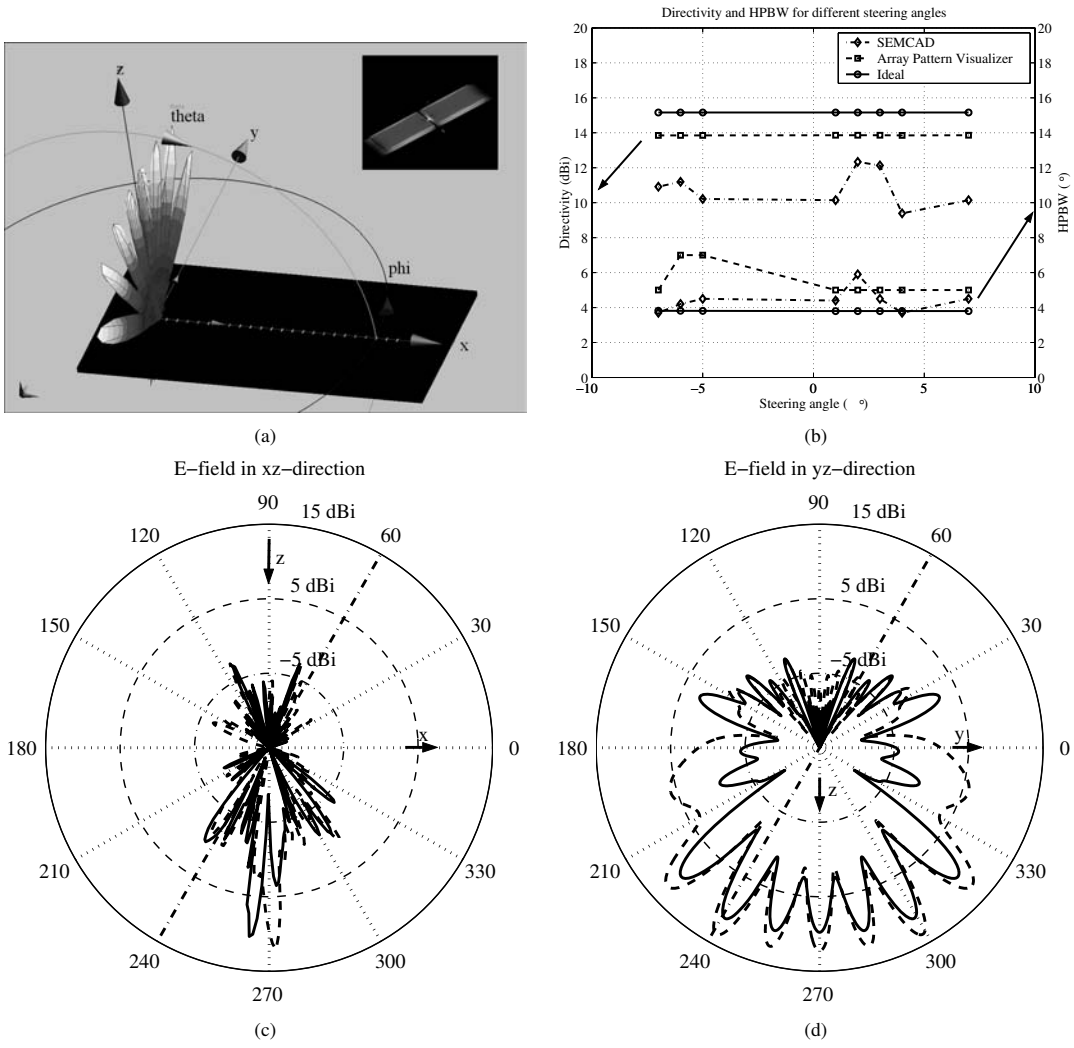

Fig. 5: (a) Radiation pattern and surface current distribution of the antenna array consisting of 24 dipole antenna patches, (b) Directivity and HPBW as a function of steering angle, (c-d) Polar plots of the E-field in vertical cuts at 24 GHz at steering angle 2 and -6 degrees

[7] ETSI TR 102 263 V1.1.2, *Electromagnetic compatibility and Radio spectrum Matters (ERM); Road Transport and Traffic Telematics (RTTT); Radio equipment to be used in the 77 GHz to 81 GHz band; System Reference Document for automotive collision warning Short Range Radar*, European Telecommunications Standards Institute, Feb. 2004.

[8] Australian Communications Authority, *A review of automotive radar systems - devices and regulatory frameworks.*

[9] 47cfr15.253, *The FCC rules and regulations are codified in Title 47 of the Code of Federal Regulations*, Code of Federal Regulations, Oct. 2005.

[10] ETSI EN 302 288-1, *Electromagnetic compatibility and Radio spectrum Matters (ERM); Short Range Devices; Road Transport and Traffic Telematics (RTTT); Short range radar equipment operating in the 24 GHz range; Part 1: Technical requirements and methods of measurement*, European Telecommunications Standards Institute, Dec. 2005.

[11] I. Gresham, N. Jain, T. Budka, A. Alexanian, N. Kinayman, B. Ziegner, S. Brown, and P. Steacker, "A Compact Manufacturable 76-77 GHz Radar Module for ACC Applications," *IEEE Transactions on Microwave Theory and Techniques*, vol. 49, no. 1, pp. 44–58, Jan. 2001.

[12] A. Kawakubo, S. Tokoro, Y. Yammada, K. Kuroda, and T. Kawasaki, "Electronically-Scanning Millimeter-Wave RADAR for Forward Object Detection," *SAE Technical Paper Series*, 2004-01-1122.

[13] Prismark Discovery Series, "Automotive radar, cruising at 77 while stopping crashes at 24," *Prismark Partners LLC*, Dec. 2004.

[14] C. A. Balanis, *Antenna Theory: Analysis and Design*, 2nd ed. New York: John Wiley and Sons, Inc., 1996.

[15] SEMCAD, http://www.semcad.com.

[16] J. Granholm and K. Woelders, "Dual Polarization Stacked Microstrip Patch Antenna Array With Very Low Cross-Polarization," *IEEE Transactions on Antennas and Propagation*, no. 10, Oct. 2001.

[17] N. Chamberlain, L. Amaro, E. Oakes, R. Hodges, S. Spitz, and P. A. Rosen, "Microstrip Patch Antenna Panel for Large Aperture L-band Phased Array," *IEEE Conference Aerospace*, pp. 1185–1192, Mar. 2005.

[18] P. Salonen and H. Hurme, "A Novel Fabric WLAN Antenna For Wearable Applications," *IEEE Antennas and Propagation Society International Symposium*, pp. 700 – 703, June 2003.

[19] J. Kraus and R. Marhefka, "Array Pattern Visualizer," http://esl.eng.ohio-state.edu/ rjm/antennas/standalone.htm.